A facile method for effective doping of Tb^{3+} into ZnO nanocrystals†

Shulin Ji, Liangliang Yin, Guodong Liu, Lide Zhang and Changhui Ye*

Received (in Cambridge, UK) 3rd February 2009, Accepted 20th February 2009
First published as an Advance Article on the web 11th March 2009
DOI: 10.1039/b902282a

A technical challenging issue in rare-earth ion doping in ZnO nanocrystals has been tackled in this communication by a novel isocrystalline core–shell protocol, and the fabricated ZnO:Tb^{3+}/ZnO core/shell nanocrystals showed efficient doping and excellent optical properties.

Recent years have seen unprecedented studies on optical properties of semiconductor nanocrystals,[1–3] among which rare-earth ions doped semiconductors have attracted much attention due to their distinct optical properties.[4–7] However, due to the small size (< 10 nm) where the quantum confinement effect manifests itself, the nanocrystals show a self-purification effect[8] and the dopant atoms are generally impelled to the outer surface of the nanocrystals, which, unfortunately, makes the doping inefficient. Moreover, as a consequence of a high surface to volume ratio inherent to the nanocrystals, there exist on the surface numerous dangling bonds[9,10] and defect states[11] that usually act as trapping centers for charge carriers and play a rather deleterious role on the optical properties. Recently, efforts have been devoted to develop synthetic approaches to improving optical properties of doped nanocrystals by suppressing energy loss processes at the surface of the nanocrystals,[12–14] however, for rare-earth ions doped ZnO nanocrystals, work is still lacking. Since this type of materials have many significant applications in light emitting devices, bioassay, photonics and so on, developing a general, facile chemical method for efficient doping of rare-earth ions into ZnO nanocrystals is essential for their application.

ZnO, a wide bandgap (3.37 eV) semiconductor with a large exciton binding energy (60 meV), is an important optical material which may find applications in light-emitting devices, lasers, photocatalysts, solar cells, and so on.[15,16] In the past decade, ZnO nanocrystals doped with transition metal ions have attracted worldwide attention since room-temperature ferromagnetic properties have both been theoretically predicted and experimentally proved.[17,18] Consequently, this material system has been deemed as one of the most promising candidates for spintronics. To improve doping and eliminate surface defects, we report in this communication an isocrystalline core–shell (ICS) protocol, which involves epitaxial growth of an undoped shell layer of the same semiconductor material on the doped nanocrystal surface, to synthesize ZnO:Tb^{3+}/ZnO core–shell nanocrystals. A mild post-annealing is very effective for obtaining internally doped nanocrystals with few surface defects. In addition to the improved photoluminescence performance, the effective rare-earth ion doping in ZnO nanocrystals also induces enhanced response to visible light that is essential for solar cells.[19] Last but not least, Tb^{3+} ion may act as a local structural probe[20,21] to determine the locations of the dopant ions in the nanocrystals owing to the sensitivity of the rare-earth ions to local crystallography and bonding conditions.

The doped nanocrystals were synthesized in solution (for experimental details, see ESI†).[22] The wurtzite structure of doped ZnO nanocrystals [ZnO:Tb^{3+}(4.0 at%)] was identified by powder XRD [Fig. 1(d)] and electron diffraction [Fig. 1(b)]. No diffraction peaks related with terbium phases besides those of ZnO (JCPDS No. 89-1397) were detected by XRD under annealing in air below 400 °C. When the annealing temperature was raised to above 500 °C, the Tb_4O_7 phase began to appear and the crystallite size grew larger. For the 400 °C annealed sample, the crystallite size determined for the (002) reflection of the XRD pattern by using the Debye–Scherrer equation is 14.1 nm while the average size is 9.1 ± 0.9 nm as determined

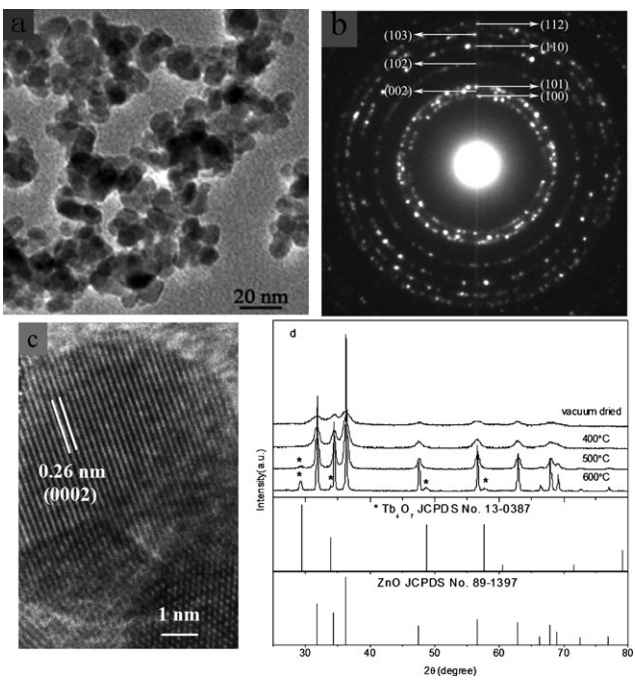

Fig. 1 (a) TEM image, (b) diffraction pattern, and (c) HRTEM image of ZnO:Tb^{3+}(4.0 at%)/ZnO core–shell nanocrystals annealed in air at different temperatures for 2 h. (d) XRD patterns of ZnO nanocrystals of different preparation conditions.

Key Laboratory of Materials Physics and Anhui Key Laboratory of Nanomaterials and Nanotechnology, Institute of Solid State Physics, Chinese Academy of Sciences, Hefei, 230031, China. E-mail: chye@issp.ac.cn; Fax: (+) 86-551-5591434; Tel: (+) 86-551-5592755

† Electronic supplementary information (ESI) available: Experimental details, Raman, and EDS spectra of samples. See DOI: 10.1039/b902282a

 This journal is © The Royal Society of Chemistry 2009

from the (110) reflection. This indicates that some of the particles were somewhat elongated along the *c*-axis which was proved by the high-resolution transmission electron microscopy (HRTEM) image in Fig 1(c). The mean diameter of the hexagonal particles ($\sim$9 nm) is in good agreement with the XRD-estimated average size of 9.1 $\pm$ 0.9 nm, while the particles before formation of the shell have an average size of 7–8 nm. A typical result should be mentioned about the absence of an interface separating the core from the shell in all investigated particles by HRTEM. This is a strong evidence of epitaxial growth of an isocrystalline shell on the surface of doped-core. The Raman spectra of pure and doped ZnO under different treatments were also recorded [Fig. S1a, ESI†], and no significant change by doping was detected, indicating that stresses and defects (if any) were not severe after doping. The size and morphology of the ICS nanocrystals is uniform according to TEM analysis [Fig. 1(a)]. Electron energy dispersion spectroscopy (EDS) analysis [Fig. S1b, ESI†] reveals the effective doping of terbium ions in ZnO with concentration close to 4%.

The absorption spectra of doped samples [ZnO:Tb^{3+} (4.0 at%)] are presented in Fig. 2. The core–shell sample exhibited ZnO band-edge absorption around 375 nm and no noticeable absorption was observed in the range of 400–800 nm before annealing. After vacuum drying, the absorption showed little increase while a small red shift of the absorption edge was observed [Fig. S2, ESI†]. These observations reveal that annealing at elevated temperature is necessary for crystallization and substitution of Tb^{3+} ions into ZnO lattices. Interaction between neighboring nanocrystals after removal of solution by vacuum drying resulted in the red shift of the spectrum. Annealing at 400 °C for 2 h without vacuum drying enhanced the visible range absorption (400–700 nm), however, with vacuum drying and annealing the absorption increased dramatically. The increase of absorption in the visible range can be attributed to the Tb^{3+} doping effect. In practice, 4f–4f electron transitions make a substantial contribution to the optical absorption in the visible range,[21] which will be further detailed in the following section. In contrast to the 'core–shell annealed sample', the 'core annealed' sample exhibited a more intense visible range absorption (170% higher for the latter at 450 nm when the spectra are normalized at 300 nm), which can be partially attributed to the formation of an amorphous phase of Tb_4O_7 according to the literature.[23] In addition, the ICS nanocrystals with Tb^{3+} dopant of 4.0 at% has a more intense optical absorption in the visible range than those with 1.0 at% dopant (17% increase at 450 nm when the spectra are normalized at 300 nm), implying that it might still be possible to further increase the optical absorption by using a larger doping concentration [Fig. S2, ESI†].

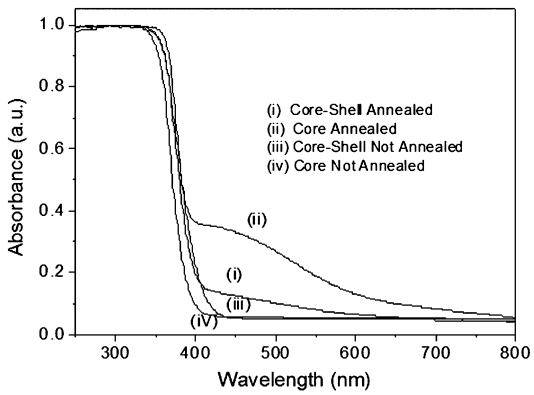

Fig. 2 Absorption spectra of doped samples under different treatments, the curves were normalized at 300 nm.

PL spectra of the products (ZnO:Tb^{3+} (4.0 at%)) are displayed in Fig. 3(a). Before annealing, both 'core not annealed' and 'core–shell not annealed' nanocrystals only show a broad green emission (under 325 nm excitation) that is the defect related PL, well-documented in the literature. However, after annealing in air at 400 °C for 2 h, characteristic intra-4f transition luminescence was observed in addition to near band-edge emission (NBE) of ZnO. The additional PL peaks implied the good crystallinity and effective doping of the annealed samples compared with the non-annealed samples. Moreover, after normalization, it can be seen clearly from the upper two curves that the intensity ratio of the rare-earth ion related peaks to the NBE peak increases dramatically for the core–shell sample. This observation is an indication of more efficient energy transfer from host material (ZnO) to guest ions (Tb^{3+}) and better optical properties of the core–shell sample (ICS nanocrystals). To study the excitation response of the samples, PLE spectra were recorded by monitoring the emission wavelength of 548 nm according to Fig. 3(a). In Fig. 3(b), the 'not annealed' samples contain two strong peaks at $\sim$250, 370 nm, and one weak peak at $\sim$488 nm. The two strong peaks correspond to the charge transfer state (CTS) and inner 4f–4f transition, respectively, and the weak peak can be ascribed to the $^7F_6 \rightarrow {}^5D_4$ transition.[24,25] For the 'core-annealed' sample, the inner 4f–4f transition peak further

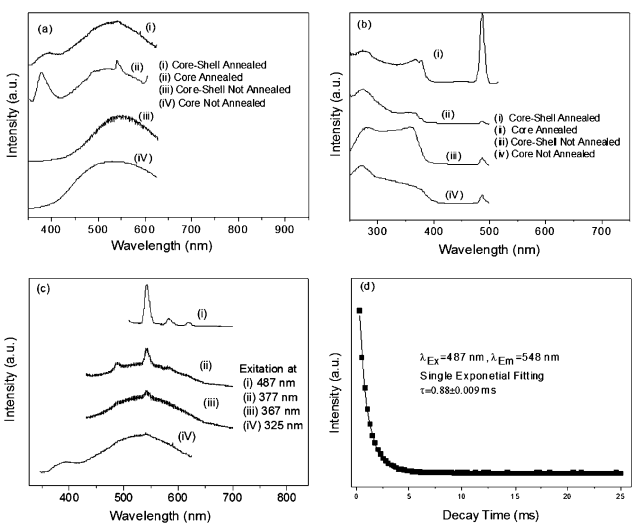

Fig. 3 (a) PL spectra under 325 nm excitation, (b) PLE spectra by monitoring 548 nm emission, of different samples. (c) PL spectra under different excitations according to the PLE peaks in (b), and (d) PL decay curves of the 548 nm emission under 487 nm excitation, of the 'core–shell annealed' sample. Curves in (a)–(c) were normalized and are shifted for clarity.

splits into two peaks, with the longer wavelength peak being much weaker than the shorter wavelength one. The PLE spectrum for the 'core–shell annealed' sample is, however, drastically different from all the other samples discussed previously. The two most striking features of the PLE spectrum are the very intense peak at ~488 nm and the double peaks at ~366 and 377 nm with similar intensity. The intense $^7F_6 \rightarrow {}^5D_4$ transition is a definite indicator of the effective doping and good crystallinity of the host material. The more interesting observation is the splitting of the 4f–4f transitions and the gaining of intensity of the longer wavelength peak. Because the 4f–4f transitions are rather closely spaced, they are generally not separable due to either ineffective doping or polydispersity of crystal size of the host nanocrystals. Trying to assign a particular transition to a broad PLE peak is, therefore, unreliable. However, for our 'core–shell annealed' sample we can unambiguously assign these two PLE peaks at ~366 and 377 nm to $^7F_6 \rightarrow {}^5G_6$ and $^7F_6 \rightarrow {}^5D_3$ transitions, respectively.[26] The visibility of peak splitting of the 4f–4f transition and the gain in intensity of the lower lying transition ($^7F_6 \rightarrow {}^5D_3$) are another definite indicator of the effective doping and good crystallinity of our ICS nanocrystals. To further confirm energy transfer from host (ZnO) to guest (Tb^{3+}) as pointed out in the previous section, PL spectra of the 'core–shell annealed' sample under 325, 367, 377, 487 nm excitations were examined [Fig. 3(c)] according to the PLE spectrum [Fig. 3(b)]. When the excitation wavelength is changed from 325 nm to longer regions (367 and 377 nm), both the emission from ZnO and Tb^{3+} are present. For an even longer excitation wavelength of 487 nm, which is not sufficient to excite PL from ZnO, only emission from Tb^{3+} is observed. It is noteworthy that 325 nm excitation does not correspond to a particular transition to Tb^{3+}, however, typical emissions from Tb^{3+} are still present. In order to investigate recombination kinetics of the excited electrons, PL decay behavior of the $^5D_4$–$^7F_5$ transition emission (~548 nm) was studied [Fig. 3(d)]. The decay curve was well fitted by a single exponential decay function with a decay time ~0.88 ms. This decay time agrees well with that reported by Saitoh and co-workers of 1.06 ms for Y_2O_3 whiskers doped with 3.8 at% of Tb^{3+} ions.[27] The small variation is possibly due to a difference in crystal size and doping level. Although Tb^{3+} ions might diffuse in the ICS crystal, and even partially into the shell, nonetheless, few of them (if any) reside on the surface, considering the single exponential decay behavior of the PL, where the single exponential decay of PL is a clear indication of few defects on the crystal surface. The effective doping of rare-earth ions in the interior of the ICS nanocrystals is the biggest advantage of our method.

In summary, by developing a novel two-step method, isocrystalline core–shell nanocrystals of ZnO:Tb^{3+}@ZnO were synthesized. The ICS nanocrystals demonstrated effective doping and good crystallinity, as revealed by photoluminescence and excitation spectra. Efficient energy transfer from host material (ZnO) to guest ions (Tb^{3+}) was observed. ICS nanocrystals with effective doping of rare-earth ions in the interior and excellent optical properties make them ideal candidates in the application of light emitting devices.

This work was supported by National Natural Science Foundation of China (Grant No. 10874183), Anhui Provincial Key Laboratory Special Fund, and the Presidential Scholarship Special Fund.

Notes and references

1 A. P. Alivisatos, *J. Phys. Chem.*, 1996, **100**, 13226.
2 P. V. Radovanovic, N. S. Norberg, K. E. McNally and D. R. Gamelin, *J. Am. Chem. Soc.*, 2002, **124**, 15192.
3 F. V. Mikulec, M. Kuno, M. Bennati, D. A. Hall, R. G. Griffin and M. G. Bawendi, *J. Am. Chem. Soc.*, 2000, **122**, 2532.
4 Z. Zhou, T. Komori, T. Ayukawa, H. Yukawa, M. Morinaga, A. Koizumi and Y. Takeda, *Appl. Phys. Lett.*, 2005, **87**, 091109.
5 A. S. Pereira, M. Peres, M. J. Soares, E. Alves, A. Neves, T. Monteiro and T. Trindade, *Nanotechnology*, 2006, **17**, 834.
6 J. Lin, Y. Huang, J. Zhang, J. M. Gao, X. X. Ding, Z. X. Huang, C. C. Tang, L. Hu and D. F. Chen, *Chem. Mater.*, 2007, **19**, 2585.
7 K. Kömpe, H. Borchert, J. Storz, A. Lobo, S. Adam, T. Möller and M. Haase, *Angew. Chem., Int. Ed.*, 2003, **42**, 5513.
8 G. M. Dalpian and J. R. Chelikowsky, *Phys. Rev. Lett.*, 2006, **96**, 226802.
9 V. Sudarsan, S. Sivakumar, F. C. J. M. van Veggel and M. Raudsepp, *Chem. Mater.*, 2005, **17**, 4736.
10 X. Bai, H. W. Song, G. H. Pan, Z. X. Liu, S. Z. Lu, W. H. Di, X. G. Ren, Y. Q. Lei, Q. L. Dai and L. B. Fan, *Appl. Phys. Lett.*, 2006, **88**, 143104.
11 H. S. Peng, H. W. Song, B. J. Chen, S. Z. Lu and S. H. Huang, *Chem. Phys. Lett.*, 2003, **370**, 485.
12 U. K. Gautam, L. S. Panchakarla, B. Dierre, X. S. Fang, Y. Bando, T. Sekiguchi, A. Govindaraj, D. Golberg and C. N. R. Rao, *Adv. Funct. Mater.*, 2009, **19**, 131.
13 C. Louis, S. Roux, G. Ledoux, L. Lemelle, P. Gillet, O. Tillement and P. Perriat, *Adv. Mater.*, 2004, **16**, 2163.
14 P. V. Radovanovic and D. R. Gamelin, *J. Am. Chem. Soc.*, 2001, **123**, 12207.
15 M. H. Huang, S. Mao, H. Feick, H. Q. Yan, Y. Y. Wu, H. Kind, E. Weber, R. Russo and P. D. Yang, *Science*, 2001, **292**, 1897.
16 M. Law, L. E. Greene, J. C. Johnson, R. Saykally and P. D. Yang, *Nat. Mater.*, 2005, **4**, 455.
17 D. A. Schwartz, K. R. Kittilstved and D. R. Gamelin, *Appl. Phys. Lett.*, 2004, **85**, 1395.
18 H. Wang, Y. Chen, H. B. Wang, C. Zhang, F. J. Yang, J. X. Duan, C. P. Yang, Y. M. Xu, M. J. Zhou and Q. Li, *Appl. Phys. Lett.*, 2007, **90**, 052505.
19 P. V. Kamat, *J. Phys. Chem. C*, 2008, **112**, 18737.
20 J. W. Wang, H. W. Song, B. J. Sun, X. G. Ren, B. J. Chen and W. Xu, *Chem. Phys. Lett.*, 2003, **379**, 507.
21 H. W. Song and J. W. Wang, *J. Lumin.*, 2006, **118**, 220.
22 E. A. Meulenkamp, *J. Phys. Chem. B*, 1998, **102**, 5566.
23 M. Sekita, Y. Miyazawa, S. Morita, H. Sekiwa and Y. Sato, *Appl. Phys. Lett.*, 1994, **65**, 2380.
24 G. Lakshminarayana and S. Buddhudu, *Mater. Chem. Phys.*, 2007, **102**, 181.
25 C. F. Wu, Y. H. Wang and W. J. Liu, *J. Solid State Chem.*, 2006, **179**, 4047.
26 R. Boyn, *Phys. Status Solidi B*, 1988, **148**, 11.
27 H. Najafov, Y. Satoh, S. Ohshio, A. Kato and H. Saitoh, *Jpn. J. Appl. Phys.*, 2004, **43**, 7111.

 This journal is © The Royal Society of Chemistry 2009